JOURNAL OF CATALYSIS 64, 295–302 (1980)

# The Catalytic Oxidation of Propylene

## VIII. An Investigation of the Kinetics over $Bi_2Mo_3O_{12}$, $Bi_2MoO_6$, and $Bi_3FeMo_2O_{12}$

L. DAVID KRENZKE* AND GEORGE W. KEULKS

*Department of Chemistry, Laboratory for Surface Studies, University of Wisconsin–Milwaukee, Milwaukee, Wisconsin 53201*

Received October 1, 1979; revised February 8, 1980

The kinetics of propylene oxidation have been investigated over the temperature range of 325 to 475°C. The apparent activation energies changed from 15 to 18 kcal/mole at high temperature (>400°C) to 43–53 kcal/mole at lower temperatures. The reaction orders for both oxygen and propylene also changed with temperature. It was found that these changes in the kinetic parameters could be completely explained in terms of the coupled kinetics of catalyst reduction and reoxidation.

## INTRODUCTION

The kinetics of propylene oxidation have received considerably less attention in the literature than the mechanistic or catalyst development studies. There are several reasons for this. First, the kinetics appear to be quite complex. The reported propylene and oxygen dependencies of acrolein formation vary from first order in $C_3H_6$ and zero order in $O_2$ for bismuth molybdate (*1*) to zero order in $C_3H_6$ and first order in $O_2$ for cuprous oxide (*2*). The apparent activation energies also vary over a wide range, from ~12 to ~35 kcal/mole. Second, there appears to be no simple relationship between the observed kinetics and the reaction mechanism. For example, the reported $C_3H_6$ and $O_2$ dependencies for bismuth molybdate are exactly the reverse of the dependencies reported for cuprous oxide and yet the mechanism of acrolein formation is identical over both catalysts (*3*, *4*).

Some of the above difficulties arise from the use of poorly defined catalysts and narrow ranges of reaction conditions which overlap poorly with the conditions used in mechanistic studies. Consequently for this report we have chosen well-characterized and stable selective oxidation catalysts and determined the kinetic parameters for both partial and complete oxidation over a wide temperature range. These kinetics will then be discussed in terms of the mechanistic data given in the previous paper (*5*).

## EXPERIMENTAL

### *1. Catalyst Preparations*

The procedures for preparing pure $Bi_2Mo_3O_{12}$, $Bi_2MoO_6$, and $Bi_3FeMo_2O_{12}$ have been previously reported (*5*). The surface areas of the catalyst were determined by the BET method using an Adsorptomat (American Instrument, Inc.).

### *2. Apparatus*

All the experiments were carried out in a single-pass flow reactor at atmospheric pressure. The reactor consisted of 8-mm Pyrex tubing as a preheat volume and catalyst chamber. To minimize the possibility of a homogeneous reaction in the postcatalytic zone (*6*), a section of 1-mm capillary tubing was used below the catalyst bed.

The reactor was heated in a tubular furnace, controlled by a Thermoelectric R-100 temperature controller. The temperature of

* Present address: Union Oil of California, Research Department, P.O. Box 76, Brea, California 92621



0021-9517/80/080295-08$02.00/0

the reaction was monitored by a dual-junction $\frac{1}{16}$-in. sheathed type K thermocouple inserted directly into the catalyst bed. One thermocouple was connected to the temperature controller and the other to a calibrated Simpson pyrometer.

The feed gases, oxygen (Airco, 99.6%), propylene (Matheson, C.P. grade), and helium (Airco, 99.99%), were used without further purification. The individual gas flows were controlled by Tylan mass flow controllers, Model FC-260.

The feed gas composition and product distribution were analyzed by an in-line gas chromatograph (Porapak R column ($\frac{1}{4}$ in. × 6 ft at 140°C). The peak areas and component concentrations were obtained from a Spectra-Physics Autolab System I Computing integrator.

### 3. *Procedure*

In order to obtain accurate kinetic data, several precautions were taken. First, the size of the catalyst charge was kept small ($Bi_2Mo_3O_{12}$, 0.10 g; $Bi_2MoO_6$, 0.05 g; and $Bi_3FeMo_3O_{12}$, 0.075 g). This served to reduce the possibility of developing temperature gradients in the catalyst bed. Second, all of the kinetic measurements on a given catalyst were made on the same catalyst charge with periodic activity checks to determine if any deactivation had occurred. Third, the catalysts were lined-out for several hours to be sure a steady-state reaction was reached before any kinetic data were taken. Fourth, the conversion level was kept below 5% so that diffferential rate data could be obtained directly.

In order to maintain a low conversion level with a fixed catalyst charge over a wide temperature range (325–475°C) the total flow rate was varied between 20 and 100 STP $cm^3$/min. The reaction orders for propylene and oxygen in both selective and nonselective oxidation were determined at seven different temperatures. When determining the pressure dependence of propylene, the oxygen partial pressure was held constant at 0.3 atm while decreasing the propylene partial pressure from 0.3 atm to 0.1 atm. When determining the pressure dependence of oxygen, the propylene partial pressure was held constant at 0.1 atm while decreasing the oxygen partial pressure from 0.3 atm to 0.1 atm. The reaction order with respect to propylene and oxygen was calculated from plots of ln rate (acrolein or $CO_2$ formation) versus ln of the pressure of the reactant being varied.

## RESULTS

The surface areas of the catalyst used in this study are given in Table 1. These areas were used to calculate the specific rate constants shown in the Arrhenius plots.

The periodic activity checks made during the accumulation of the kinetic data showed no loss in activity for any of the catalysts. The problem in this respect was with $Bi_2MoO_6$. This catalyst is very active and at temperatures above 460°C with a propylene partial pressure of 0.3 atm, there is a tendency for the reaction temperature to become uncontrollable. This generally results in the irreversible loss of catalyst activity. Consequently, the maximum temperature used for the kinetic measurements with this catalyst was 450°C.

The reaction orders of oxygen and propylene for acrolein and carbon dioxide formation are given in Table 2. The reaction orders of both propylene and oxygen vary with temperature. The order of propylene in both $C_3H_4O$ and $CO_2$ formation decreases with decreasing temperature. The order in oxygen generally increases with decreasing temperature for acrolein formation but is a positive value at all temperatures for carbon dioxide formation.

The specific rate constant for acrolein and carbon dioxide formation was calcu-

TABLE 1

BET Surface Areas

| Catalyst | Area ($m^2$/g) |
|---|---|
| $Bi_2Mo_3O_{12}$ | 1.6 |
| $Bi_2MoO_6$ | 2.1 |
| $Bi_3FeMo_2O_{12}$ | 9.4 |

TABLE 2

Reaction Orders for Propylene Oxidation

| Catalyst | Temperature (°C) | $C_3H_4O$ formation | | $CO_2$ formation | |
|---|---|---|---|---|---|
| | | $C_3H_6$ | $O_2$ | $C_3H_6$ | $O_2$ |
| $Bi_2Mo_3O_{12}$ | 475 | 1 | 0 | 1 | 0.4 |
| | 450 | 1 | 0 | 1 | 0.4 |
| | 425 | 1 | 0 | 1 | 0.4 |
| | 400 | 1 | 0 | 1 | 0.4 |
| | 375 | 0.7 | 0 | 0.7 | 0.4 |
| | 350 | 0 | 0 | 0 | 0.4 |
| | 325 | 0 | 0 | 0 | 0.4 |
| $Bi_2MoO_6$ | 450 | 1 | 0 | 1 | 0.4 |
| | 435 | 1 | 0 | 1 | 0.4 |
| | 420 | 1 | 0 | 1 | 0.4 |
| | 400 | 0.8 | 0 | 0.8 | 0.4 |
| | 375 | 0.2 | 0.4 | 0.2 | 0.4 |
| | 350 | 0 | 0.4 | 0 | 0.4 |
| | 325 | 0 | 0.4 | 0 | 0.4 |
| $Bi_3FeMo_2O_{12}$ | 475 | 1 | 0 | 1 | 0.4 |
| | 450 | 1 | 0 | 1 | 0.4 |
| | 425 | 1 | 0 | 1 | 0.5 |
| | 400 | 1 | 0.3 | 1 | 0.7 |
| | 375 | 1 | 0.4 | 1 | 0.8 |
| | 350 | 0.5 | 1 | 0.7 | 1 |
| | 325 | 0.2 | 1 | 0.6 | 1 |

lated from the specific rate of formation, the observed reaction orders, and the partial pressures of oxygen and propylene. A number of experiments were made at each

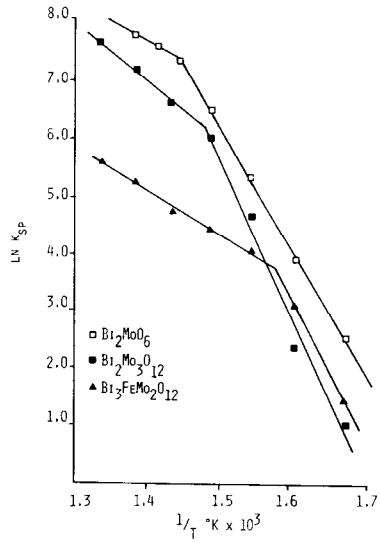


FIG. 1. Arrhenius plot for $C_3H_4O$ formation.

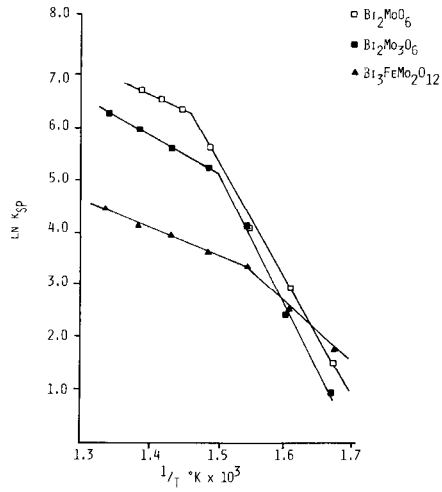


FIG. 2. Arrhenius plot for $CO_2$ formation.

temperature and as expected they yielded essentially the same value for the specific rate constant. Therefore, an average value was used for the Arrhenius plots of acrolein formation, Fig. 1, and carbon dioxide formation, Fig. 2. The Arrhenius plots for $C_3H_4O$ and $CO_2$ formation yield two intersecting lines. The slopes of these lines were determined by a linear regression analysis and the resulting energies of activation are given in Table 3.

## DISCUSSION

The observed reaction kinetics for acrolein and carbon dioxide formation appear to be quite complex. The pressure dependencies of both oxygen and propylene change with temperature. The Arrhenius plots

TABLE 3

Apparent Energies of Activation for $C_3H_4O$ and $CO_2$ Formation

| Catalyst | Temperature range (°C) | $E_A$ (kcal/mole) | |
|---|---|---|---|
| | | $C_3H_4O$ | $CO_2$ |
| $Bi_2Mo_3O_{12}$ | >410 | 18 | 13 |
| | <410 | 53 | 49 |
| $Bi_2MoO_6$ | >419 | 15 | 12 |
| | <419 | 43 | 43 |
| $Bi_3FeMo_2O_{12}$ | >379 | 15 | 10 |
| | <379 | 48 | 23 |

yield two intersecting lines, representing a high activation energy in the low-temperature region and a low activation energy in the high-temperature region. Before discussing the origins of these kinetic parameters, several relevant points from the previous paper (*5*) which described the reaction mechanism will be restated:

1. The observation of a secondary discrimination effect for the oxidation of propylene-2,3,3,3-$d_4$ and the participation of multiple layers of lattice oxygen in the formation of acrolein at 350, 400, and 450°C strongly suggest that acrolein is formed exclusively via the redox mechanism over this temperature range. Therefore, the change in the kinetic parameters is not due to a change in the reaction mechanism.

2. The observation of similar kinetic parameters, kinetic isotope effects, and oxygen-18 incorporation for both acrolein and $CO_2$ over the bismuth molybdates strongly suggests that $CO_2$ is formed by the consecutive oxidation of acrolein. At low conversions as used in these studies, this statement is more realistically meant to imply that the $CO_2$ actually is formed from an adsorbed precursor of acrolein or from a stable surface intermediate produced after the formation of the allylic species. With $Bi_3FeMo_2O_{12}$, on the other hand, $CO_2$ is formed by both the consecutive and parallel pathways and involves both lattice and adsorbed oxygen.

3. The observation of a full primary isotope effect for acrolein formation during the oxidation of propylene-2,3,3,3-$d_4$ at 450°C strongly suggests that the rate-limiting step at high temperatures is the abstraction of an allylic hydrogen. The observation of less than a full primary isotope effect for acrolein formation during the oxidation of propylene-2,3,3,3-$d_4$ at 350°C suggests that some process other than allyl formation is the rate-limiting step at lower temperatures.

The basic concept of a redox cycle for oxidation was suggested by Mars and van Krevelan (*7*) for the oxidation of naphthalene. It now is relatively well accepted that the redox mechanism functions for a number of selective oxidation catalysts, especially the bismuth molybdate system. Indeed, a number of investigators (*8–10*) have shown quantitatively that product formation and catalyst reduction proceed simultaneously. It was also shown that the rate of this reaction decreases rapidly with an increasing degree of catalyst reduction. Consequently, in order to maintain a continuous catalytic reaction, the catalyst oxygen must be continually replenished via reoxidation from the gas phase.

With this concept in mind, Eqs. (1) and (2) can be written as follows:

$$\frac{-d[C_3H_6]}{dt} = k_R P_{C_3}^x \Theta_{ox}, \qquad (1)$$

where

$k_R$ = rate constant for catalyst reduction
$P_{C_3}$ = partial pressure of propylene
$x$ = reaction order of propylene for catalyst reduction
$\Theta_{ox}$ = fraction of sites which are fully oxidized;

$$\frac{-d[O_2]}{dt} = k_{ox} P_{O_2}^y (1 - \Theta_{ox}), \qquad (2)$$

where

$k_{ox}$ = rate constant for catalyst reoxidation
$P_{O_2}$ = partial pressure of oxygen
$y$ = reaction order of oxygen for catalyst reoxidation
$(1 - \Theta_{ox})$ = fraction of sites which are reduced.

These equations indicate that the rate of catalyst reduction, which is equal to the rate of propylene oxidation for bismuth molybdate catalysts, is dependent upon the number of oxidized sites and that this parameter is controlled both by the reduction and reoxidation processes. Under steady-state reaction conditions, the flow of oxygen into the catalyst equals the flow of oxygen out of the catalyst as oxygenated

products. Therefore, Eqs. (1) and (2) may be equated and solved for $\Theta_{ox}$, yielding:

$$\Theta_{ox} = \frac{k_{ox}P^{y}_{O_2}/k_R P^{x}_{C_3}}{1 + (k_{ox}P^{y}_{O_2}/k_R P^{x}_{C_3})}. \quad (3)$$

Figure 3 gives the graphical representation of the relationship between the fraction of sites which are oxidized and the ratio of the rates of reoxidation and reduction. This figure indicates that the number of oxidized sites is almost constant when the rate of reoxidation is much greater than the rate of reduction. On the other hand, when the rate of reoxidization is much less than the rate of reduction, the number of oxidized sites is very sensitive to changes in the rate of reoxidation.

The relationship between the rate of propylene oxidation and the ratio of the rates of catalyst reoxidization and reduction can be clearly shown by substituting Eq. (3) for the value of $\Theta_{ox}$ in Eq. (1), yielding:

$$\frac{-d[C_3H_6]}{dt} = k_R P^{x}_{C_3} \left[\frac{k_{OX}P^{y}_{O_2}k_R P^{x}_{C_3}}{1 + (k_{OX}P^{y}_{O_2}/k_R P^{x}_{C_3})}\right]. \quad (4)$$

Now, if $k_{ox}P^{y}_{O_2}/k_R P^{x}_{C_3} \gg 1$, Eq. (4) can be reduced to:

$$\frac{-d[C_3H_6]}{dt} = k_R P^{x}_{C_3}. \quad (5)$$

In this case, the kinetics of propylene oxidation are the same as the kinetics of catalyst reduction. On the other hand, if $k_{ox}P^{y}_{O_2}/k_R P^{x}_{C_3} \ll 1$, Eq. (4) is reduced to:

$$\frac{-d[C_3H_6]}{dt} = k_{ox}P^{y}_{O_2}. \quad (6)$$

Now the kinetics of propylene oxidation are controlled by the kinetics of catalyst reoxidation. Therefore, the observed kinetics of propylene oxidation would be expected to change drastically if, by changing reaction conditions, the process was shifted from a reduction-limited region to a reoxidation-limited region. This transition would involve not only a change in activation energy, but also a change in the reaction orders of oxygen and propylene. In the reduction-limited region (Eq. (5)), the reaction has a positive order in propylene and is zero order in oxygen, whereas in the reoxidation-limited region (Eq. (6)), the reverse

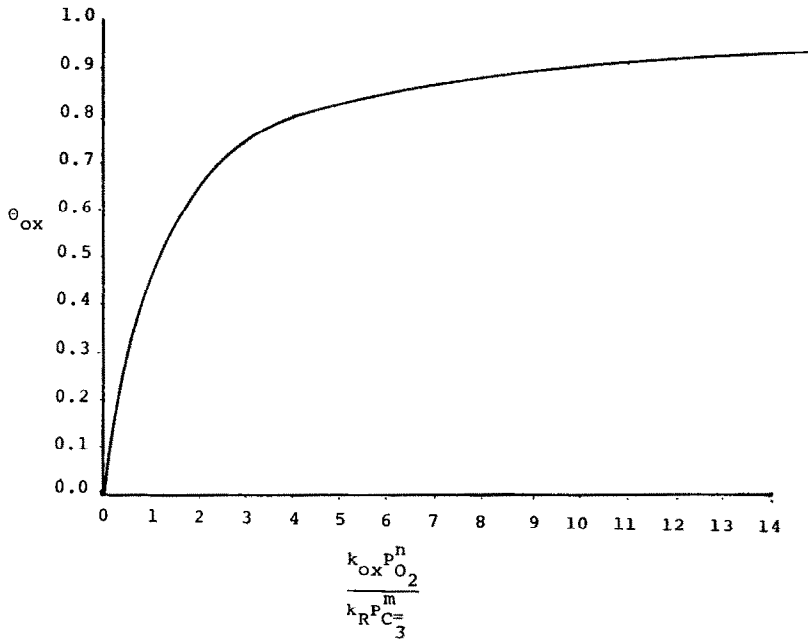


FIG. 3. Fraction of fully oxidized sites vs the ratio of the rate of reoxidation to the rate of reduction.

is true. In the transition region, the observed kinetics would be a composite of both the reduction and reoxidation kinetics. Therefore, activation energies between those of reduction and reoxidation and positive reaction orders in both reactants are possible.

The above general description of redox kinetics is in good qualitative agreement with the observed kinetics of acrolein and carbon dioxide formation, with the exception of failing to detect a positive oxygen dependency for acrolein formation at low temperatures with $Bi_2Mo_3O_{12}$. More recent work (*11*) suggests that this is due to the failure to examine lower oxygen partial pressures where the positive dependency is indeed observed. Thus, the kinetics of propylene oxidation are merely a composite of the individual kinetics for catalyst reduction and reoxidation. This concept can be supported further by making a quantitative comparison of the kinetics for these various processes. Reduction–reoxidation data are, unfortunately, available for only the $\gamma$-phase bismuth molybdate ($Bi_2MoO_6$). However, since the mechanism and major kinetic features are the same for the other molybdates, the results of this comparison can be applied to these catalysts.

The kinetics for the reduction of $Bi_2MoO_6$ with propylene and the subsequent reoxidation have been determined by Uda *et al.* (*12*) using the microbalance technique. They found that the reduction step was first order in propylene and had an activation energy of 14 kcal/mole and that reoxidation was 0.6 order in oxygen with an activation energy of 46 kcal/mole. The kinetic parameters for the reduction of $Bi_2MoO_6$ are very similar to those given for acrolein formation in the high-temperature region (first order in $C_3H_6$ and 15 kcal/mole), while the reoxidation kinetics closely match the acrolein kinetics of the low-temperature region (0.4 order in $O_2$ and 43 kcal/mole). This suggests that propylene oxidation is controlled primarily by catalyst reduction in the high-temperature region and is reoxidation limited at lower temperatures.

The close relationship between the observed propylene oxidation kinetics and the general kinetic features of a redox reaction is evident. However, this can be illustrated even more clearly by comparing the observed kinetic parameters with those predicted by the redox mechanism. Using the data of Uda *et al.* (*12*), the relationship given in Eq. 4, and the temperatures and reactant partial pressures used experimentally with $Bi_2MoO_6$, theoretical reaction velocities for propylene oxidation can be calculated. Substituting these calculated rates into the empirical rate equation, rate = $k[C_3H_6]^m[O_2]^n$, allows the theoretical apparent reaction orders and rate constants to be determined. The calculated reaction orders for propylene and oxygen are compared with the observed values at seven temperatures in Table 4. It can be seen that the redox kinetics accurately predict the observed change in the reaction orders with temperature. The temperature dependency of the calculated rate constants was also determined and is shown in Fig. 4. This is essentially identical to the experimental Arrhenius plots for acrolein and carbon dioxide formation over $Bi_2MoO_6$. Both the acti-

TABLE 4

Comparison of the Reaction Orders Calculated from Redox Kinetics with The Observed Reaction Orders for $C_3H_6$ Oxidation

| Temperature, (°C) | Over $Bi_2MoO_6$ | | | | Calculated values | |
|---|---|---|---|---|---|---|
| | $C_3H_4O$ formation | | $CO_2$ formation | | | |
| | $C_3H_6$ | $O_2$ | $C_3H_6$ | $O_2$ | $C_3H_6$ | $O_2$ |
| 450 | 1 | 0 | 1 | 0.4 | 1 | 0 |
| 435 | 1 | 0 | 1 | 0.4 | 1 | 0 |
| 420 | 1 | 0 | 1 | 0.4 | 1 | 0 |
| 400 | 0.8 | 0 | 0.8 | 0.4 | 0.6 | 0.2 |
| 375 | 0.2 | 0.4 | 0.2 | 0.4 | 0.4 | 0.3 |
| 350 | 0 | 0.4 | 0 | 0.4 | 0.2 | 0.5 |
| 325 | 0 | 0.4 | 0 | 0.4 | 0 | 0.6 |

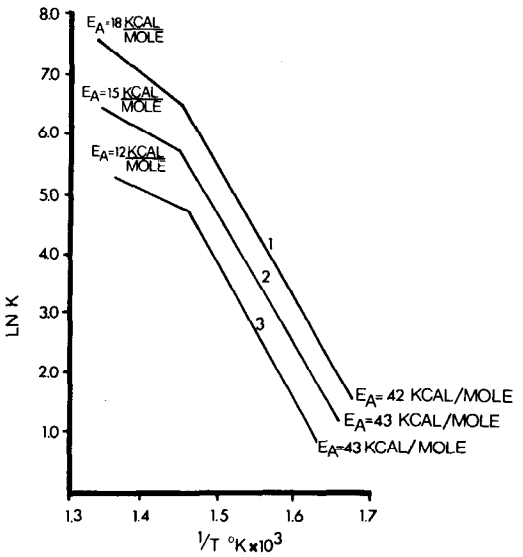


FIG. 4. Arrhenius plot for $C_3H_6$ oxidation over $Bi_2MoO_6$ calculated from redox kinetics. (1) Calculated curve; (2) experimental curve for $C_3H_4O$ formation from Fig. 1; (3) experimental curve for $CO_2$ formation from Fig. 2.

vation energies and the inflection points are in good agreement.

The only feature not accounted for by the redox kinetics is the positive oxygen dependency for $CO_2$ formation in the high-temperature (reduction-limited) region over the bismuth molybdates. The positive order in oxygen is not unexpected for $Bi_3FeMo_2O_{12}$ since $CO_2$ is formed from adsorbed oxygen as well as lattice oxygen. However, with the bismuth molybdates only lattice oxygen is involved. In the previous article (*5*) it was suggested that the complete combustion region over $Bi_2Mo_6O_{12}$ and $Bi_2MoO_6$ was initiated by a charge transfer process which resulted in the activation of an oxide to an $O^-$ ion. Sancier *et al.* (*13*) studied the kinetics of the charge transfer processes which occurred during the reduction and reoxidation of bismuth molybdate catalysts. They found that during reoxidation, the charge transfer process exhibited a 0.5-order dependence on oxygen pressure. This is essentially the same oxygen dependency observed for $CO_2$ formation in the high-temperature region where the redox reaction is no longer controlled by reoxidation. Consequently, it seems reasonable to assume that the charge transfer process which occurs during reoxidation and the process which initiates carbon dioxide formation are closely related. This concept is supported by the work of Anshiz *et al.* (*14*). They oxidized butane and hexene over zinc oxide and cuprous oxide in the presence of oxygen-18 and concluded that molecular oxygen did not directly participate in $CO_2$ formation but that it promoted the decomposition of surface compounds.

It was noted in the Introduction that the maximum reported value of energy of activation for acrolein formation was ~35 kcal/mole. This is significantly lower than the low-temperature activation energies of 43–53 kcal/mole given in Table 3. This discrepancy arises from the method of calculation. Most researchers have assumed first-order kinetics at all temperatures and have calculated their rate constants accordingly. If this procedure were used with the data in this report, the low-temperature activation energies for acrolein formation over all three molybdate catalysts would be ~36 kcal/mole. Consequently, the activation energies reported here are in good agreement with those previously reported in the literature.

In conclusion, it appears that the kinetics of propylene oxidation over $Bi_2Mo_3O_{12}$, $Bi_2MoO_6$, and $Bi_3FeMo_2O_{12}$ can be completely explained in terms of the coupled kinetics of catalyst reduction and reoxidation.

## REFERENCES

1. Adams, C. R., Voge, H. H., Morgan, C. Z., and Armstrong, W. E., *J. Catal.* **3**, 379 (1964); Keulks, G. W., Rosynek, M. P., and Daniel, C., *Ind. Eng. Chem. Prod. Res. Develop.* **10**, 138 (1971).
2. Isaev, O. V., and Margolis, L. Y., *Kinet. Katal.* **1**, 237 (1960).
3. Adams, C. R., and Jennings, T. J., *J. Catal.* **2**, 63 (1963).
4. Adams, C. R., and Jennings, T. J., *J. Catal.* **3**, 549 (1964).
5. Krenzke, L. D., and Keulks, G. W., *J. Catal.* **61**, 316 (1980).

6. Keulks, G. W., and Daniel, C., *J. Catal.* **24,** 529 (1971).
7. Mars, P., and van Krevelen, D. W., *Chem. Eng. Sci. Suppl.* **3,** 41 (1954).
8. Aykan, D., *J. Catal.* **12,** 281 (1968).
9. Batist, P. A., Prette, H. J., and Schuit, G. C. A., *J. Catal.* **15,** 267 (1969).
10. Peacock, J. M., Parker, A. J., Ashmore, P. G., and Hockey, J. A., *J.Catal.* **15,** 398 (1968).
11. Monnier, J. M., Ph.D. Dissertation, University of Wisconsin–Milwaukee, 1978.
12. Uda, T., Lin, T., and Keulks, G. W., *J. Catal.*, **62,** 26 (1980).
13. Sancier, K. M., Aoshima, A., and Wise, H., *J. Catal.* **34,** 257 (1974).
14. Anshiz, A. G., Sokolvskii, V. D., Boreskov, G. K., and Borinin, A. I., *React. Kinet. Catal. Lett.* **7,** 87 (1977).